

1
2
3
4
5
6
7
8
9
10
11
12
13
14
15
16
17
18
19
20
21
22
23
24
25
26
27
28
29
30
31
32
33
34
35
36
37
38
39
40
41
42
43
44
45
46
47
48
49
50
51
52
53
54
55
56
57
58
59
60
61
62
63
64
65

Dynamic adhesion energy between surfaces connected by molecular bonds and its application to peel test

Yuan Lin^{1,*}, Shuhuai Yao², and Qiang Xu¹

¹ Department of Mechanical Engineering, The University of Hong Kong

Hong Kong SAR, China

² Department of Mechanical Engineering, Hong Kong University of Science and Technology

Hong Kong SAR, China

*Corresponding author: ylin@hku.hk

April 28, 2010

Abstract

We consider the energy needed to separate two surfaces connected by molecular bonds, whose formation and breakage can be described by the classical rate equation. We find that this adhesion energy is strongly rate-dependent due to the chemical kinetics involved. Two cases where the separation between surfaces grows linearly, or exponentially, with respect to time are studied in detail, scaling relations between the adhesion energy and separation speed, or the exponential factor, are derived in each case. As an example of application, the peel test of a membrane in adhesive contact with a substrate is also studied. We will show that findings obtained here can be

1
2
3
4
5
6
7
8
9 directly used to predict the relationship between the applied tension and the peeling
10 velocity, which is of central interest to this type of experiment.
11
12
13

14 **1 Introduction**

15
16
17 In biological adhesion, two bodies are usually brought together by bonds formed between
18 adhesion molecules on the two surfaces [1]. These adhesion molecules are proteins with
19 long chains [2], which make them compliant and deformable under load [3]. One important
20 feature about these bonds is that each of them will break eventually if one waits long enough.
21 On the other hand, any broken bond can reform if proximity is maintained. As a result, the
22 rupture force of a single bond, or multiple parallel bonds, strongly depends on the loading
23 rate [4, 5]. Similarly, for a vesicle adhering to a substrate, the maximum force that can
24 be achieved when pulling the vesicle away from the substrate is also rate-dependent [6]-[8].
25 Besides rupture force, sometimes we are more interested in the adhesion energy between
26 two surfaces, a key quantity in the analysis of crack propagation or peel test as will be
27 demonstrated later. In this study, our focus is on the influence of the chemical kinetics of
28 bond formation, as well as breakage, on the adhesion energy.
29
30
31
32
33
34
35
36
37
38
39

40 The amount of work needed for creating new surfaces is of special interest in fracture
41 and contact mechanics [9, 10]. This quantity is often referred to as the surface energy or
42 fracture energy. The rate-dependent fracture energy of materials has long been studied
43 both experimentally and theoretically by different researchers. The rate sensitivity may
44 originate from the bulk viscoelastic behavior of the material [11, 12], or from the plastic
45 flow near the crack tip [13, 14]. For surfaces connected by molecular bonds, Schallamach
46 [15] studied the influence of the chemical kinetics of bond association/dissociation on the
47
48
49
50
51
52
53
54
55
56
57
58
59
60
61
62
63
64
65

1
2
3
4
5
6
7
8
9
10
11
12
13
14
15
16
17
18
19
20
21
22
23
24
25
26
27
28
29
30
31
32
33
34
35
36
37
38
39
40
41
42
43
44
45
46
47
48
49
50
51
52
53
54
55
56
57
58
59
60
61
62
63
64
65

dynamic friction of rubbers. Schallamach's approach was adopted by Chaudhury [16] to explain the rate-dependency of the fracture energy of polymer-glass interface. Here, we conduct a systematic investigation on the variation of adhesion energy with respect to how two surfaces connected by molecular bonds are separated. This issue is important in, for example, studying cell locomotion where cell-substrate attachment needs to be released at the rear end of a motile cell while nascent adhesions have to be formed continuously at the front end [17], hence an accurate estimation of the adhesion energy is undoubtedly one of the keys for us to evaluate the energy consumption associated with cell movement, a quantity of great biological, as well as physical, significance.

2 Dynamic adhesion energy

Consider two flat surfaces in adhesive contact by forming molecular bonds between them, as depicted in Figure 1. Let A be the areal density of the unbroken bonds, and denote A_0 as the total adhesion molecule density which is a constant. The formation and breakage of bonds can then be described by the first order rate equation as

$$\frac{dA}{dt} = -k_- A + k_+(A_0 - A) \tag{1}$$

where k_+ and k_- are the so-called association and dissociation rates. Let y be the separation of two surfaces when subjected to a pulling force F , see Figure 1. If bonds are treated as linear springs then the force acting on a single bond is

$$f = k_s y \tag{2}$$

1
2
3
4
5
6
7
8
9
10
11
12
13
14
15
16
17
18
19
20
21
22
23
24
25
26
27
28
29
30
31
32
33
34
35
36
37
38
39
40
41
42
43
44
45
46
47
48
49
50
51
52
53
54
55
56
57
58
59
60
61
62
63
64
65

Figure 1: Diagram of two surfaces in adhesive contact by forming molecular bonds between them.

where k_s is the spring constant representing the deformability of the bond. Suppose that we are conducting a displacement-controlled experiment, i.e. the separation y as a function of time is controlled. If equilibrium is always enforced during separation, the pulling force F then must take the form

$$F(t) = k_s y(t) A(t). \tag{3}$$

The adhesion energy W_{ad} , which, by definition, equals to the work done by separating two surfaces completely, can be expressed as

$$W_{ad} = \int_0^\infty F dy. \tag{4}$$

To evaluate this quantity, the relationship between separation y and reaction rates must first be prescribed. Following Bell [18], here the dissociation rate k_- of a bond is assumed to increase exponentially with the force acting on it, that is

$$k_- = k_-^0 e^{fa/k_B T}. \quad (5)$$

Here k_-^0 is the dissociation rate under vanishing force and $k_B T$ is the thermal energy. a is a constant, in the order of 0.1-1 nm, representing the distance between the transition state and the bonding state of the bond. The forward rate k_+ may also depend on the separation y as, for example, explored in [16] and [19]. However, in order to derive the essential results in the simplest manner, k_+ is taken to be a constant here, i.e.

$$k_+ = k_+^0. \quad (6)$$

Notice that, from (5), a characteristic length y_0 arises naturally as

$$y_0 = \frac{k_B T}{k_s a}. \quad (7)$$

By introducing dimensionless variables $w = y/y_0$, $\tau = k_+^0 t$ and $\eta = A/A_0$, (1) becomes

$$\frac{d\eta}{d\tau} = -(1 + K e^w)\eta + 1 \quad (8)$$

where $K = k_-^0/k_+^0$. If the energy gained by forming a single bond is U_b then, from thermodynamics, we have $K = e^{-U_b/k_B T}$. An initial condition is needed for solving (8), here chemical equilibrium is assumed to be reached at the beginning of the separation process, that is

$$\eta(\tau = 0) = 1/(1 + K). \quad (9)$$

1
2
3
4
5
6
7
8
9 Obviously, the adhesion energy defined in (4) depends on the separation history $y(t)$, or
10 $w(\tau)$. At this point, it is informative to consider the equilibrium state solution, which can
11 be obtained by enforcing chemical equilibrium at any separation as
12
13
14

$$15 \quad \eta_0(w) = \frac{1}{1 + Ke^w} \quad (10)$$

16
17
18
19 Notice that (10) represents the solution when the separation process is infinite slow, or, from
20 thermodynamics point of view, the system undergoes a reversible process. Substitute (10)
21 into (4), the adhesion energy for the reversible, or quasi-static, process is
22
23
24
25

$$26 \quad W_0 = -\text{Li}_2(-1/K) \quad (11)$$

27
28
29 where W_0 is the dimensionless form of W_{ad} , normalized by $k_s A_0 y_0^2$. $\text{Li}_2(z)$ is the standard
30 Polylogarithm function whose value is readily to be evaluated in most mathematics softwares.
31
32 To demonstrate the dynamic effect, two cases are examined in detail here. First, we consider
33 the case where two surfaces separate with a constant speed. After that, the separation is
34 assumed to grow exponentially with respect to time in the second scenario.
35
36
37
38
39

40 **2.1 Separation increases linearly with time**

41
42
43 In this case, w is a linear function of τ , i.e.
44
45

$$46 \quad w(\tau) = v\tau. \quad (12)$$

47
48
49
50 Here v is the dimensionless separation speed, normalized by $y_0 k_+^0$. Notice that similar
51 problem has been considered by Seifert [20] in the context of finding the velocity dependence
52
53
54
55

1
2
3
4
5
6
7
8
9 of the strength of the bond. Basically, the adhesion energy discussed here corresponds to
10 the area under the force-separation curve obtained in [20]. The solution of (8) can be found
11 as
12
13

$$\eta(w) = \frac{e^{K/v}}{1+K} e^{G(w)} + \frac{e^{G(w)}}{v} \int_0^w e^{-G(\xi)} d\xi \quad (13)$$

14
15
16
17
18
19 where $G(w) = -w/v - Ke^w/v$. Notice that here η is expressed in terms of separation w .
20 Figure 2 shows how the solution deviates from $\eta_0(w)$ at different separation speeds. Clearly,
21 the difference grows as v increases. This is not surprising because as separation process
22 becomes faster the system has less time to reach chemical equilibrium and, consequently,
23 more bonds will remain unbroken at the same separation distance, see Figure 2. Recall that
24 bonds are treated as linear springs here, hence larger pulling force F must be applied to
25 sustain higher separation speed.
26
27
28
29
30
31
32
33
34
35
36
37
38
39
40
41
42
43
44
45
46
47
48

49 Figure 2: Bond densities as functions of separation distance under different separation
50 speeds. The parameter K is chosen to be 0.1.
51
52

53 The normalized adhesion energy W , $W = \frac{W_{ad}}{k_s A_0 y_0^2}$, can be determined through (4) and
54
55

1
2
3
4
5
6
7
8
9 (13). Calculation results of W , divided by W_0 , as a function of v is illustrated in Figure 3 by
10 the solid line for $K = 0.1$. To investigate the scaling relations between W and v , we proceed
11 by considering two limiting scenarios where the separation speed is either very small or very
12 large.
13
14
15
16
17
18
19
20
21
22
23
24
25
26
27
28
29
30
31
32

33 Figure 3: Adhesion energy as a function of separation speed. The solid line represents
34 numerical results and the two dashed lines correspond to asymptotic relationships as $v \rightarrow 0$
35 and $v \rightarrow \infty$. The parameter K is chosen to be 0.1.
36
37
38

39 **2.1.1 Adhesion energy under small separation speed**

40
41 For $v \ll 1$, we expect the solution of (8) to be very close to $\eta_0(w)$, see Figure 2. Following
42 standard perturbation methods, the solution $\eta(w)$ is expressed in terms of power series of v
43 as
44
45
46
47
48

$$49 \eta(w) = \eta_0(w) + v\eta_1(w) + v^2\eta_2(w) + \dots \quad (14)$$

50
51
52 Substituting (14) into (8) and matching of terms of the order of v leads to
53
54
55
56
57
58
59
60
61
62
63
64
65

$$\eta_1(w) = \frac{Ke^w}{(1 + Ke^w)^3}. \quad (15)$$

Hence the adhesion energy, defined in (4), takes the form

$$\frac{W}{W_0} \approx 1 + v \frac{-1 + (1 + K)\ln(1 + 1/K)}{-2(1 + K)\text{Li}_2(-1/K)}. \quad (16)$$

Obviously, (16) shows that the adhesion energy increases linearly with respect to the separation speed when it is small.

2.1.2 Adhesion energy under large separation speed

When $v \gg 1$, it can be shown that the second term appeared on the right hand side of (13) becomes negligible, so the adhesion energy can be evaluated as

$$W = \frac{e^{K/v}}{1 + K} \left({}_2F_2(\mathbf{a}; \mathbf{b}; -K/v)v^2 + v(K/v)^{1/v}\Gamma(1 - 1/v)[\ln(K/v) - \psi(-1/v)] \right) \quad (17)$$

where $\mathbf{a} = [-1/v, -1/v]$ and $\mathbf{b} = [1 - 1/v, 1 - 1/v]$. ${}_2F_2(\mathbf{a}; \mathbf{b}; z)$ is the Hypergeometric function, $\Gamma(z)$ is the Gamma function, and $\psi(z)$ is the PolyGamma function. As $1/v \rightarrow 0$, or equivalently $K/v \rightarrow 0$, the asymptotic form of (17) becomes

$$W \approx \frac{[\ln(K/v)]^2/2 + \gamma\ln(K/v)}{1 + K} \quad (18)$$

in which $\gamma = 0.577216$ is the Euler number. (18) suggests that, under large separation speed, the scaling relation between W and v takes the form

1
2
3
4
5
6
7
8
9
10
11
12
13
14
15
16
17
18
19
20
21
22
23
24
25
26
27
28
29
30
31
32
33
34
35
36
37
38
39
40
41
42
43
44
45
46
47
48
49
50
51
52
53
54
55
56
57
58
59
60
61
62
63
64
65

$$W^{1/2} \sim \ln(v). \tag{19}$$

The asymptotic expressions of W , as shown in (16) and (18), are illustrated in Figure 3 by the dashed lines, which clearly agree well with numerical results.

2.2 Separation increases exponentially with time

In some practical cases, like the peel test to be discussed later, it's more appropriate to assume the separation increases exponentially with time, i.e.

$$w(\tau) = e^{b\tau} - 1 \tag{20}$$

where b is called the exponential factor. Under such circumstance (8) can be rewritten as

$$\frac{d\eta}{dw} = -\frac{(1 + Ke^w)}{b(1 + w)}\eta + \frac{1}{b(1 + w)} \tag{21}$$

The solution of (21), satisfying the initial condition (9), can be found as

$$\eta(w) = \frac{e^{K\text{Ei}(1)/be}}{1 + K} e^{G(w)} + \frac{e^{G(w)}}{b} \int_0^w \frac{e^{-G(\xi)}}{1 + \xi} d\xi \tag{22}$$

where $\text{Ei}(z)$ is the so-called Exponential integral function and

$$G(w) = -[K\text{Ei}(1 + w)/e + \ln(1 + w)]/b. \tag{23}$$

It's unlikely that any closed form expression, similar to (16) or (18), of the adhesion energy W can be obtained in this case. However, notice that when b is large the second term on

1
2
3
4
5
6
7
8
9 the right hand side of (22) becomes negligible. In addition, recall the function $\text{Ei}(z)$ has the
10 following asymptotic expression
11

$$12 \quad \text{Ei}(z) \sim \frac{e^z}{z} \quad \text{as } z \rightarrow \infty. \quad (24)$$

13
14
15
16
17 In light of (24), as $b \rightarrow \infty$, a critical length w_c can be identified by enforcing $G(w_c) = -1$ as
18

$$19 \quad w_c \sim \ln(b/K). \quad (25)$$

20
21
22
23
24 Physically, the exponential decay of the bond density is so significant when $w \gg w_c$, see
25 (22), we can basically assume all bonds are broken in this range. On the other hand, for
26 $w \ll w_c$, the decay in η is very small and hence it can be treated as a constant, equal to
27 $\frac{1}{1+K}$, here. Based on these observations, the adhesion energy W can be roughly estimated
28
29
30
31 as
32

$$33 \quad W \sim \int_0^{w_c} \frac{w}{1+K} dw = \frac{[\ln(b/K)]^2}{2(1+K)} \quad (26)$$

34
35
36
37
38 Numerical results of W as a function of b for different K values are shown in Figure 4,
39 which clearly demonstrates that \sqrt{W} is indeed proportional to $\ln(b)$ as predicted by (26).
40
41 In addition, the slopes of the curves in Figure 4 also agree with (26). Hence, the validity
42
43 of (26) is verified by direct numerical simulations. Next we will show how findings obtained
44
45 here can be used in applications like the standard peel test.
46
47
48
49
50
51
52
53
54
55
56
57
58
59
60
61
62
63
64
65

1
2
3
4
5
6
7
8
9
10
11
12
13
14
15
16
17
18
19
20
21
22
23
24
25
26
27
28
29
30
31
32
33
34
35
36
37
38
39
40
41
42
43
44
45
46
47
48
49
50
51
52
53
54
55
56
57
58
59
60
61
62
63
64
65

Figure 4: Adhesion energy as a function of exponential factor b for different K values.

3 Application to peel test

Analyses in the previous section have demonstrated that the adhesion energy between two surfaces, connected by molecular bonds, strongly depends on how we separate them. In this section, we shift our attention to the peel test which is widely used to investigate the interface properties between dissimilar materials. Specifically, we want to examine whether the scaling laws obtained before can be used to predict the relationship between the applied tension and the peeling velocity which is of central interest to this kind of experiment.

The standard peel test configuration is illustrated in Figure 5, where a membrane adhering to a substrate is peeled off by applying a remote tension. Evans examined this problem by treating the adhesion between membrane and substrate as either continuous across the interface or localized at discrete points [21, 22]. Dembo and co-workers [19] extended the study by considering the formation and breakage of molecular bonds that are

1
2
3
4
5
6
7
8
9 responsible for adhesion. Here we revisit this problem from an energy balance perspective.

10 Like before, assume the adhesion between membrane and substrate is caused by molec-
11 ular bonds formed between them and denote A_0 as the areal density of adhesion molecules.
12 In addition, assume bonds have the same extension-force relationship as shown in (2), the
13 same association rate as given in (6), and a dissociation rate similar to (5) as
14
15
16
17
18
19
20
21
22
23
24
25
26
27
28
29
30
31
32
33
34
35
36

37 Figure 5: Diagram of standard peel test.
38
39
40
41

$$42 \quad k_- = k_-^0 e^{|f|a/k_B T}. \quad (27)$$

43
44 Notice that the absolute value of f is used in (27) because, as will be demonstrated later,
45 bonds may undergo compression here. It's usually helpful to nondimensionlize the problem,
46 so we proceed by normalizing any length variable by y_0 as defined in (7); time variable
47 by $1/k_+^0$; bond density by A_0 ; energy density, as well as membrane tension, by $k_s A_0 y_0^2$.
48 Now back to the peel test configuration as shown in Figure 5, the position of any point
49
50
51
52
53
54
55
56
57
58
59
60
61
62
63
64
65

1
2
3
4
5
6
7
8
9 in membrane is identified by its arch length coordinate s whereas its horizon position is
10 described by x . Assume a steady-state peeling velocity v was reached, then the coordinate \bar{s}
11 in a frame moving with the same speed, relates to s , the coordinate in the stationary frame,
12 as
13
14
15
16
17

$$18 \quad \bar{s} = s + v\tau \quad (28)$$

19
20
21 where, like before, τ is the normalized time. Since steady-state is achieved, all physical
22 quantities become invariant with respect to time in the moving frame. Following [19, 21],
23 if bonds are assumed to align themselves in the vertical direction then static equilibrium of
24 membrane requires
25
26
27
28
29

$$30 \quad \frac{d^2 C}{d\bar{s}^2} - \alpha T C + \alpha w \eta \frac{dx}{d\bar{s}} = 0 \quad (29)$$

31
32
33 and

$$34 \quad \alpha \frac{dT}{d\bar{s}} + C \frac{dC}{d\bar{s}} - \alpha w \eta \frac{dw}{d\bar{s}} = 0 \quad (30)$$

35
36
37 where w is the local membrane deflection, $\alpha = k_s A_0 y_0^4 / B$ is a dimensionless parameter, B
38 is the bending rigidity of the membrane, η is again the bond density, T is the membrane
39 tension, and C is the normalized membrane curvature defined as
40
41
42
43
44
45
46
47

$$48 \quad C = (dx/d\bar{s})(d^2 w/d\bar{s}^2) - (d^2 x/d\bar{s}^2)(dw/d\bar{s}) = (d^2 w/d\bar{s}^2)/(dx/d\bar{s}). \quad (31)$$

49
50
51 If membrane is assumed to be inextensible, which is reasonable since bending deformation
52 is much easier than stretching for membranes, then simple geometry tells us
53
54
55
56
57
58
59
60
61
62
63
64
65

$$(dx/d\bar{s})^2 + (dw/d\bar{s})^2 = 1 \quad (32)$$

In the moving frame, conservation of bonds leads to

$$-v \frac{\partial \eta}{\partial \bar{s}} - (1 + Ke^{|w|})\eta + 1 = 0 \quad (33)$$

where again $K = k_-^0/k_+^0$. At the free extremity of membrane, that is $\bar{s} \rightarrow \infty$, the following asymptotic boundary conditions must be satisfied

$$T(\bar{s}) \rightarrow T_\infty, \quad dw(\bar{s})/d\bar{s} \rightarrow \sin\theta \quad \text{as } \bar{s} \rightarrow \infty. \quad (34)$$

Here T_∞ is the applied peeling tension and θ is the peeling angle, see Figure 5. Similarly, at the attached extremity of membrane, i.e. $\bar{s} \rightarrow -\infty$, the boundary conditions are

$$w(\bar{s}) \rightarrow 0, \quad \eta(\bar{s}) \rightarrow 1/(1 + K) \quad \text{as } \bar{s} \rightarrow -\infty. \quad (35)$$

Notice that (35) means that membrane deflection dies out when moving away from the adhesion edge and going deep into the attached part. Obviously, this also implies the derivatives of w , with respect to \bar{s} , must vanish when $\bar{s} \rightarrow -\infty$, which, as will be shown later, provides us additional conditions that can be used in solving the problem numerically. Now the key question is that, for given values of remote tension T_∞ and peeling angle θ , how can we find out the steady-state peeling velocity v ?

It is unlikely that v can be determined without recourse to numerical methods. However, before doing that, it is instructive to examine the problem based on energy balance arguments. Since no other dissipation mechanism, like the fluid flow induced by mem-

brane movement, is considered here, the work done by the remote tension, in advancing the adhesion front with an infinitesimal distance, must entirely be spent to separate the membrane-substrate interface, that is

$$T_\infty(1 - \cos \theta) = W \quad (36)$$

where W is exactly the adhesion energy discussed earlier. For simplicity, let's assume the origin of the moving coordinates, i.e. $\bar{s} = 0$, locates well inside the adhesion part so approximately we have $w(\bar{s} = 0) = 0$. Notice that, once the deflection profile $w(\bar{s})$ is known, then, in a stationary reference frame, the separation history $\bar{w}(\tau)$ between the point initially located at $\bar{s} = 0$ and the substrate is simply given by

$$\bar{w}(\tau) = w(v\tau). \quad (37)$$

Hence, W can be interpreted as the work needed to detach two surfaces with a separation history given in (37). Following this argument, the minimum tension T_{cr} necessary for peeling to take place can immediately be identified by letting $v \rightarrow 0$. In that case, W is identical to W_0 as defined in (11), and (36) reduces to the well-known Young's formula

$$T_{cr} = \frac{W_0}{1 - \cos \theta} = \frac{-\text{Li}_2(-1/K)}{1 - \cos \theta} \quad (38)$$

which basically is the equilibrium condition for a stationary front, i.e. $v = 0$. When $T_\infty > T_{cr}$, the steady-state peeling speed can be directly calculated from (36) and (37) once $w(\bar{s})$ is determined. Unfortunately, here the membrane deflection profile is unknown and must be solved as part of the solution. Numerically, Dembo and co-workers used a relaxation

scheme to solve the same problem [19], here we developed an alternative shooting scheme to obtain the solution. First, notice that the membrane deflection and its derivatives will all approach zero when $\bar{s} \rightarrow -\infty$, which implies

$$d\bar{s} \approx dx, \quad C \approx d^2w/d\bar{s}^2. \quad (39)$$

Recall that bonds are assumed to behave like linear springs and align themselves in the vertical direction, hence global force equilibrium requires

$$T(-\infty) \rightarrow T_\infty \cos \theta. \quad (40)$$

Consequently, as $\bar{s} \rightarrow -\infty$, (29) reduces to

$$\frac{d^4w}{d\bar{s}^4} - \alpha T_\infty \cos \theta \frac{d^2w}{d\bar{s}^2} + \alpha w \eta = 0. \quad (41)$$

The value of k_s is estimated to be around 1-5 pN/nm [3], so y_0 , as defined in (7), is expected to be in the order of 2-10 nm. It is reasonable to believe that A_0 is in the range of 100-1000 μm^{-2} since the diameter of typical adhesion molecule, such as integrin, is about 10 nm [23]. We expect B to vary from $\sim 35k_B T$ for pure lipid bilayer membrane [1] to about $300k_B T$, a rough estimate by taking into account the cytoskeleton beneath the membrane. Hence the dimensionless parameter α is usually less than 10^{-2} , recall that $\alpha = k_s A_0 y_0^4 / B$. From (41), the membrane deflection $w(\bar{s})$ must take the asymptotic form

$$w(\bar{s}) \approx e^{\lambda_1 \bar{s}} [C_1 \cos(\lambda_2 \bar{s}) + C_2 \sin(\lambda_2 \bar{s})] \quad (42)$$

as $\bar{s} \rightarrow -\infty$. Where $\lambda_1 = \sqrt{\sqrt{\alpha/(4(1+K))} + \alpha T_\infty \cos \theta/4}$ and $\lambda_2 = \sqrt{\sqrt{\alpha/(4(1+K))} - \alpha T_\infty \cos \theta/4}$.

1
2
3
4
5
6
7
8
9 C_1 and C_2 are two constants need to be determined. Notice that (42) is valid as long as α
10 is small so that the parameter λ_2 defined above is a real number. Similarly, the asymptotic
11 expressions of bond density and membrane tension can be found as
12
13

$$14 \quad \eta(\bar{s}) \approx \frac{1}{1+K} + e^{\lambda_1 \bar{s}} [D_1 \cos(\lambda_2 \bar{s}) + D_2 \sin(\lambda_2 \bar{s})] \quad (43)$$

15
16
17
18
19 and

$$20 \quad T(\bar{s}) \approx T_\infty \cos \theta \quad (44)$$

21
22
23 where $D_1 = \frac{K}{1+K} \frac{-(1+K+v\lambda_1)C_1+v\lambda_2 C_2}{(1+K+v\lambda_1)^2+(v\lambda_2)^2}$ and $D_2 = \frac{K}{1+K} \frac{-v\lambda_2 C_1-(1+K+v\lambda_1)C_2}{(1+K+v\lambda_1)^2+(v\lambda_2)^2}$. We must point
24 out that higher order terms, compared to $e^{\lambda_1 \bar{s}}$ as $\bar{s} \rightarrow -\infty$, are neglected in (39) and
25 (42)-(44).
26
27
28
29
30

31
32 Based on these asymptotic results, a shooting scheme is developed here as follows.
33 First, we choose a starting left boundary, say $\bar{s} = \bar{s}_0$, and set the membrane deflection at
34 this point to be $w(\bar{s}_0) = w_0$. Hence for arbitrarily chosen values of C_1 and v , (42)-(44)
35 provide us all the necessary initial conditions at \bar{s}_0 which allow us to integrate (29)-(33)
36 along the coordinate \bar{s} . Notice that the other constant C_2 can be determined from w_0 , \bar{s}_0
37 and C_1 . Next, Newton's method [24] is employed to find the correct combinations of C_1 and
38 v such that the asymptotic conditions (34) are satisfied at the right computational boundary
39 $\bar{s} = \bar{s}_\infty$. During computation, w_0 is taken to be small whereas \bar{s}_∞ is chosen to be large. To
40 make sure the numerical results are accurate, we keep decreasing w_0 , while increasing \bar{s}_∞ ,
41 until the solution becomes insensitive to them.
42
43
44
45
46
47
48
49

50
51 Choosing $\alpha = 10^{-4}$, $K = 0.1$, $\theta = \pi/3$ and $T_\infty/T_{cr} = 2$, the membrane deflection
52 profile is shown in Figure 6 by the solid line. The normalized peeling velocity v in this
53
54
55
56
57
58
59
60
61
62
63
64
65

1
2
3
4
5
6
7
8
9
10
11
12
13
14
15
16
17
18
19
20
21
22
23
24
25
26
27
28
29
30
31
32
33
34
35
36
37
38
39
40
41
42
43
44
45
46
47
48
49
50
51
52
53
54
55
56
57
58
59
60
61
62
63
64
65

Figure 6: Membrane deflection profile. Parameters chosen here are $\alpha = 10^{-4}$, $K = 0.1$, $\theta = \pi/3$ and $T_\infty/T_{cr} = 2$.

case is found to be around 20.5. Distributions of bond density and membrane tension are shown in Figure 7. Similar to what have been reported in [21] and [19], when moving from $\bar{s} \rightarrow -\infty$ to $\bar{s} \rightarrow \infty$, membrane actually undergoes negative deflections near the adhesion edge before it curves away from the substrate exponentially which causes the breakage of all bonds. The scheme introduced above provides us a robust tool to evaluate the peeling velocity for a given set of parameters. Nevertheless, it is still very helpful if some kind of simple formula can be derived to predict the relationship between the applied tension T_∞ and the peeling speed v , which is of central interest to the peel test. Actually, based on a large set of numerical simulations, a purely empirical formula was proposed in [19] to serve this purpose. Here, on the basis of the scaling relations obtained in the previous section, we try to derive similar formulas from energy arguments.

Notice that a characteristic length Δ in the problem can be identified as

1
2
3
4
5
6
7
8
9
10
11
12
13
14
15
16
17
18
19
20
21
22
23
24
25
26
27
28
29
30
31
32
33
34
35
36
37
38
39
40
41
42
43
44
45
46
47
48
49
50
51
52
53
54
55
56
57
58
59
60
61
62
63
64
65

Figure 7: Bond density and membrane tension distributions. Parameters chosen here are identical to those in Figure 6.

$$\Delta = \frac{1}{\sqrt{\sqrt{\alpha/(4(1+K))} + \alpha T_\infty \cos\theta/4}} \quad (45)$$

which roughly sets the length scale with which all physical quantities vary along the arch coordinate \bar{s} . As pointed out earlier, numerical results show that the membrane curves away from the substrate exponentially with respect to \bar{s} , see Figure 6. Here, we try to approximate the membrane deflection profile as

$$w(\bar{s}) \approx \begin{cases} e^{\bar{s}/\Delta} - 1 & \text{if } \bar{s} \geq 0; \\ 0 & \text{if } \bar{s} < 0. \end{cases} \quad (46)$$

In which, obviously, the negative deflection part is neglected. The deflection profile predicted by (46), for $w > 0$ only, is shown in Figure 6 by the dashed line. Notice that the point

1
2
3
4
5
6
7
8
9 corresponding to $\bar{s} = 0$ in (46) can be chosen arbitrarily, here its position in Figure 6 is picked
10 in such a way that the best fit between (46) and the computed deflection profile is achieved.
11 Clearly, (46) has captured the main features of the real deflection profile. Comparisons
12 between (46) and simulation results for other parameter values have been conducted and
13 good agreements have also been achieved (data not shown here). In light of (37), the peeling
14 velocity can be estimated by (36) where the adhesion energy W is calculated by taking the
15 separation history as
16
17
18
19
20
21
22
23

$$24 \quad \bar{w}(\tau) = e^{v\tau/\Delta} - 1 \quad (47)$$

25
26 which is almost identical to that in (20). The only difference is the parameter b appeared
27 in (20) is replaced by v/Δ in (47). In addition, notice that Δ , defined in (45), is insensitive
28 to the applied tension T_∞ when α is small which is usually the case as discussed before. In
29 light of these observations, (26) and (36) tell us that
30
31
32
33
34
35

$$36 \quad \ln(v/K) \sim [2(1+K)T_\infty(1-\cos\theta)]^{1/2} \quad (48)$$

37
38 Clearly, (48) means that, for a fixed peeling angle θ , the logarithm of the peeling velocity
39 v is proportional to the square-root of the applied tension T_∞ . Choosing $\alpha = 10^{-4}$ and
40 $\theta = \pi/3$, peeling velocity as a function of the applied tension is shown in Figure 8. Indeed,
41 the scaling relationship indicated by (48) was observed for different K values, ranging from
42 10^{-3} to 1. Similarly, results corresponding to $\alpha = 10^{-3}$ and $\alpha = 10^{-5}$ also agree with (48)
43 (data not shown here).
44
45
46
47
48
49

50 It's interesting to point out that experimental observations suggested that the square-
51 root of the fracture energy of polymer-glass interface is indeed proportional to the logarithm
52
53
54
55
56
57
58
59
60
61
62
63
64
65

1
2
3
4
5
6
7
8
9
10
11
12
13
14
15
16
17
18
19
20
21
22
23
24
25
26
27
28
29
30
31
32
33
34
35
36
37
38
39
40
41
42
43
44
45
46
47
48
49
50
51
52
53
54
55
56
57
58
59
60
61
62
63
64
65

of the crack propagation velocity [16], exactly following (48). However, we must also point out the problem of crack propagation is different from the peel test considered here, so that experiment did not directly corroborate our findings. Theoretical analyses, similar to that presented here, have also been conducted to explain the rate-dependency in the fracture energy of polymer materials [16, 25].

Figure 8: Peeling velocity as a function of the applied tension. Parameters chosen here are $\alpha = 10^{-4}$ and $\theta = \pi/3$.

4 Concluding remarks

In this paper, the adhesion energy between surfaces connected by molecular bonds is considered. We showed that the adhesion energy strongly depends on how the surfaces are separated due to the chemical kinetics involved in bond formation and breakage. Two cases where separation increases linearly, or exponentially, with respect to time are examined in detail. Scaling relations between the adhesion energy and the separation speed, or the exponential factor, are derived for each case. As an application, the standard peel test of a

1
2
3
4
5
6
7
8
9
10
11
12
13
14
15
16
17
18
19
20
21
22
23
24
25
26
27
28
29
30
31
32
33
34
35
36
37
38
39
40
41
42
43
44
45
46
47
48
49
50
51
52
53
54
55
56
57
58
59
60
61
62
63
64
65

membrane adhering to a substrate is studied. Based on energy balance arguments, a scaling relationship between the applied tension and the steady-state peeling velocity is obtained which agrees well with numerical results.

We hope that findings obtained here can be used to guide the design of future experiments, as well as being tested by them. In addition, we believe this work might be useful in studying other important problems like the locomotion of biological cells or the rolling of leukocytes along the vascular wall during inflammation. In cell locomotion, for example, membrane needs to be peeled away from the extracellular matrix (ECM) continuously at the trailing edge of motile cells, hence knowing the relationship between the adhesion energy and peeling velocity, identical to the cell speed in this case, should be important in evaluating the total energy consumption associated with cell movement, a quantity of great physical, as well as biological, interest.

Acknowledgment

Y. Lin wants to acknowledge the support by the Seed Funding Programme for Basic Research from The University of Hong Kong (Project No. 200809159003).

References

[1] D. Boal. 2002. *Mechanics of the Cell*. Cambridge University, Cambridge.

[2] B. Alberts, D. Bray, J. Lewis, M. Raff, K. Roberts, and J. D. Watson. 1989. *Molecular Biology of the Cell* (2nd ed). Garland Publishing, New York and London.

- 1
2
3
4
5
6
7
8
9 [3] B.T. Marshall, K.K., Sarangapani, J. Wu, M.B. Lawrence, R.P. McEver, and C. Zhu.
10 2006. Measuring molecular elasticity by atomic force microscope cantilever fluctuations.
11 Biophysical Journal 90, 681-692.
12
13
14
15 [4] E. Evans, and K. Ritchie. 1999. Strength of a weak bond connecting flexible polymer
16 chains. Biophysical Journal 76, 2439-2447.
17
18
19 [5] U. Seifert. 2000. Rupture of multiple parallel molecular bonds under dynamic loading.
20 Physical Review Letters 84, 2750-2753.
21
22
23 [6] K. Prechtel, A. R. Bausch, V. Marchi-Artzner, M. Kantslehner, H. Kessler, and R.
24 Merkel. 2002. Dynamic force spectroscopy to probe adhesion strength of living cells.
25 Physical Review Letters 89, 028101.
26
27
28 [7] A. Boulbitch. 2003. Enforced unbinding of biomembranes whose mutual adhesion is
29 mediated by a specific interaction. European Biophysical Journal 31, 637-2642.
30
31
32 [8] Y. Lin, and L. B. Freund. 2007. Forced detachment of a vesicle in adhesive contact with
33 a substrate. International Journal of Solids and Structures 44, 1927-1938.
34
35
36 [9] A. A. Griffith. 1920. The phenomenon of rupture and flow in solids. Philosophical
37 Transactions of the Royal Society (London) A221, 163-198.
38
39
40 [10] K. L. Johnson, K. Kendall, and A. D. Roberts. 1971. Surface energy and the contact
41 of elastic solids. Proceedings of the Royal Society (London) A324, 301-313.
42
43
44 [11] R. M. Christensen. 1982. Theory of Viscoelasticity: An Introduction. Academic Press,
45 New York.
46
47
48
49
50
51
52
53
54
55
56
57
58
59
60
61
62
63
64
65

- 1
2
3
4
5
6
7
8
9 [12] J. A. Greenwood, and K. L. Johnson. 1981. The Mechanics of Adhesion of Viscoelastic
10 Solids. *Philosophical Magazine A* 43, 697-711.
11
12
13 [13] P. S. Lam, and L. B. Freund. 1985. Analysis of dynamic growth of a tensile crack in an
14 elastic-plastic material. *Journal of the Mechanics and Physics of Solids* 33, 153-167.
15
16
17 [14] A. T. Zehnder, and A. J. Rosakis. 1990. Dynamic fracture initiation and propagation
18 in 4340 steel under impace loading. *International Journal of Fracture* 43, 271-285.
19
20
21 [15] A. Schallamach. 1963. A Theory of Dynamic Rubber Friction. *Wear* 6, 375-382.
22
23
24 [16] M. K. Chaudhury. 1999. Rate-Dependent Fracture at Adhesive Interface. *J. Phys.*
25 *Chem. B* 103, 6562-6566.
26
27
28 [17] P.A. DiMilla, K. Barbee, and D.A. Lauffenburger. 1991. Mathematical model for the
29 effects of adhesion and mechanics on cell migration speed. *Biophysical Journal* 60, 15-37.
30
31
32 [18] G. I. Bell. 1978. Models for the specific adhesion of cells to cells. *Science* 200, 618-627.
33
34
35 [19] M. Dembo, D. C. Torney, K. Saxman, and D. Hammer. 1988. The Reaction-Limited
36 Kinetics of Membrane-to-Surface Adhesion and Detachment. *Proceedings of the Royal*
37 *Society of London B* 234, 55-83.
38
39
40 [20] U. Seifert. 2002. Dynamic strength of adhesion molecules: role of rebinding and self-
41 consistent rates. *Europhysics Letters* 58, 792-798.
42
43
44 [21] E. Evans. 1985. Detail mechanics of membrane-membrane adhesion and separation. I.
45 Continuum of molecular cross-bridges. *Biophysical Journal* 48, 175-183.
46
47
48 [22] E. Evans. 1985. Detail mechanics of membrane-membrane adhesion and separation. II.
49 Discrete kinetically trapped molecular cross-bridges. *Biophysical Journal* 48, 185-192.
50
51
52
53
54
55
56
57
58
59
60
61
62
63
64
65

1
2
3
4
5
6
7
8
9
10
11
12
13
14
15
16
17
18
19
20
21
22
23
24
25
26
27
28
29
30
31
32
33
34
35
36
37
38
39
40
41
42
43
44
45
46
47
48
49
50
51
52
53
54
55
56
57
58
59
60
61
62
63
64
65

[23] R.O. Hynes. 1987. Integrins: a family of cell surface receptors. *Cell* 48, 549-554.

[24] W. H. Press, S. A. Teukolsky, W. T. Vetterling, and B. P. Flannery. 1992. Numerical recipes in FORTRAN. The art of scientific computing, 2nd ed. Cambridge University, Cambridge.

[25] C. Hui, T. Tang, Y. Lin, and M. K. Chaudhury. 2004. Failure of Elastomeric Polymers Due to Rate Dependent Bond Rupture. *Langmuir* 20, 6052-6064.

Figure1
[Click here to download Figure: diag.eps](#)

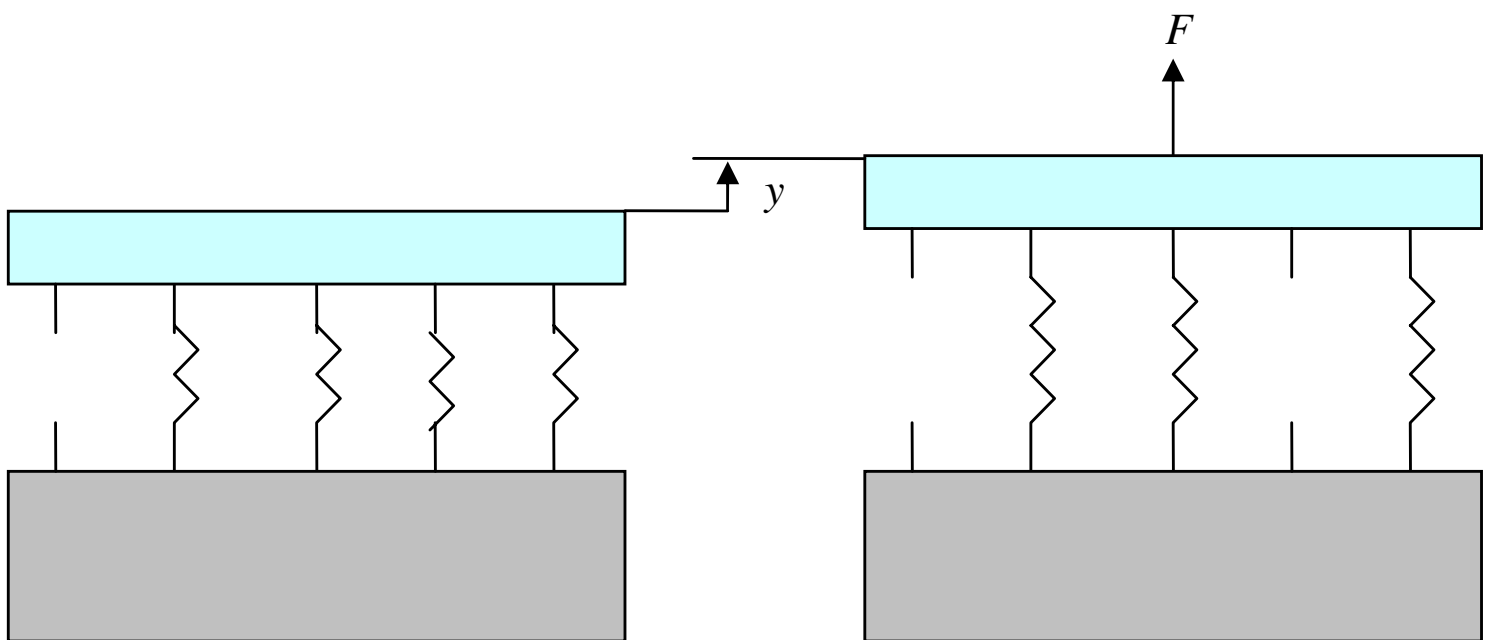


Figure2
[Click here to download Figure: eta_vs_w.eps](#)

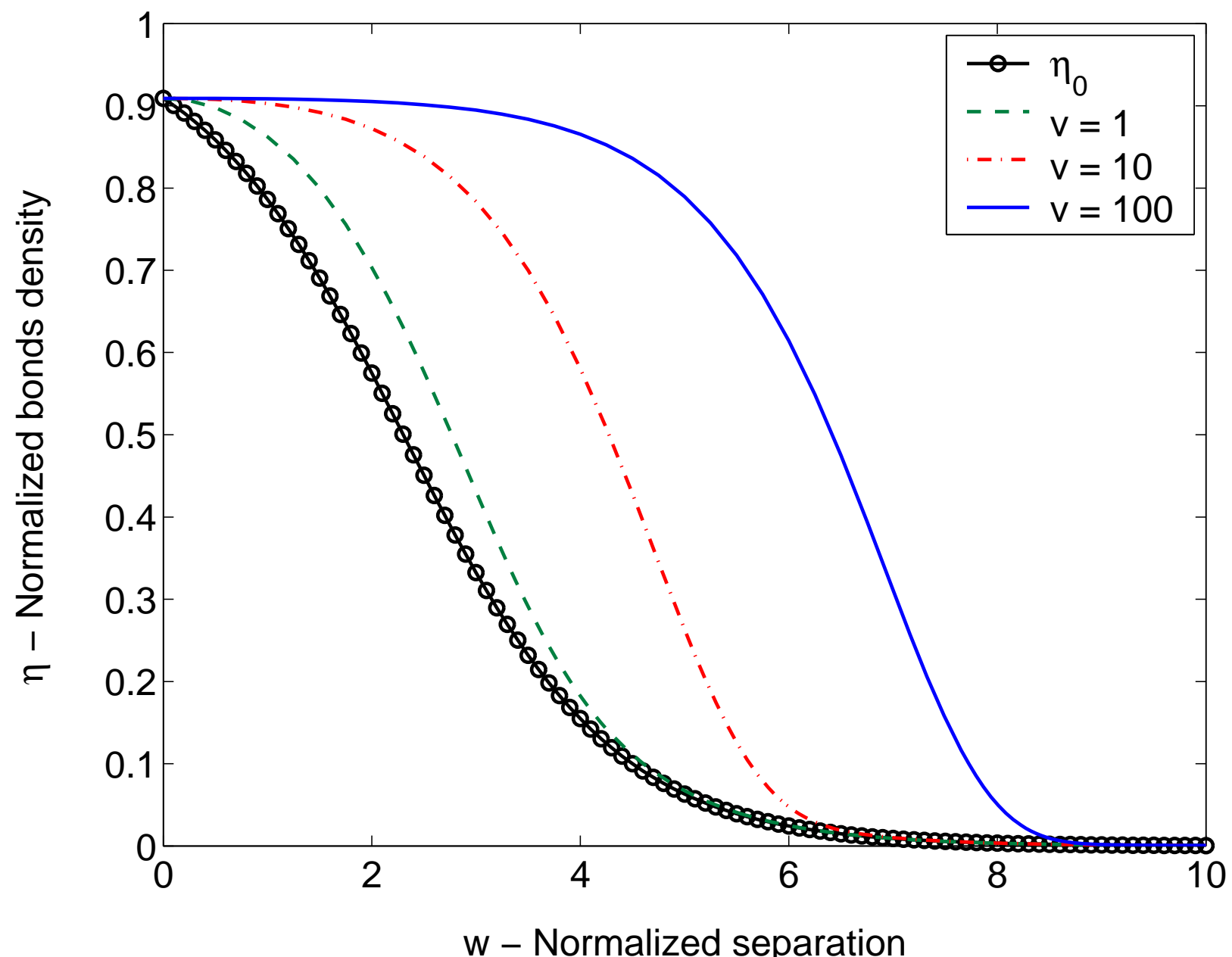


Figure3
[Click here to download Figure: Eng_vs_vel.eps](#)

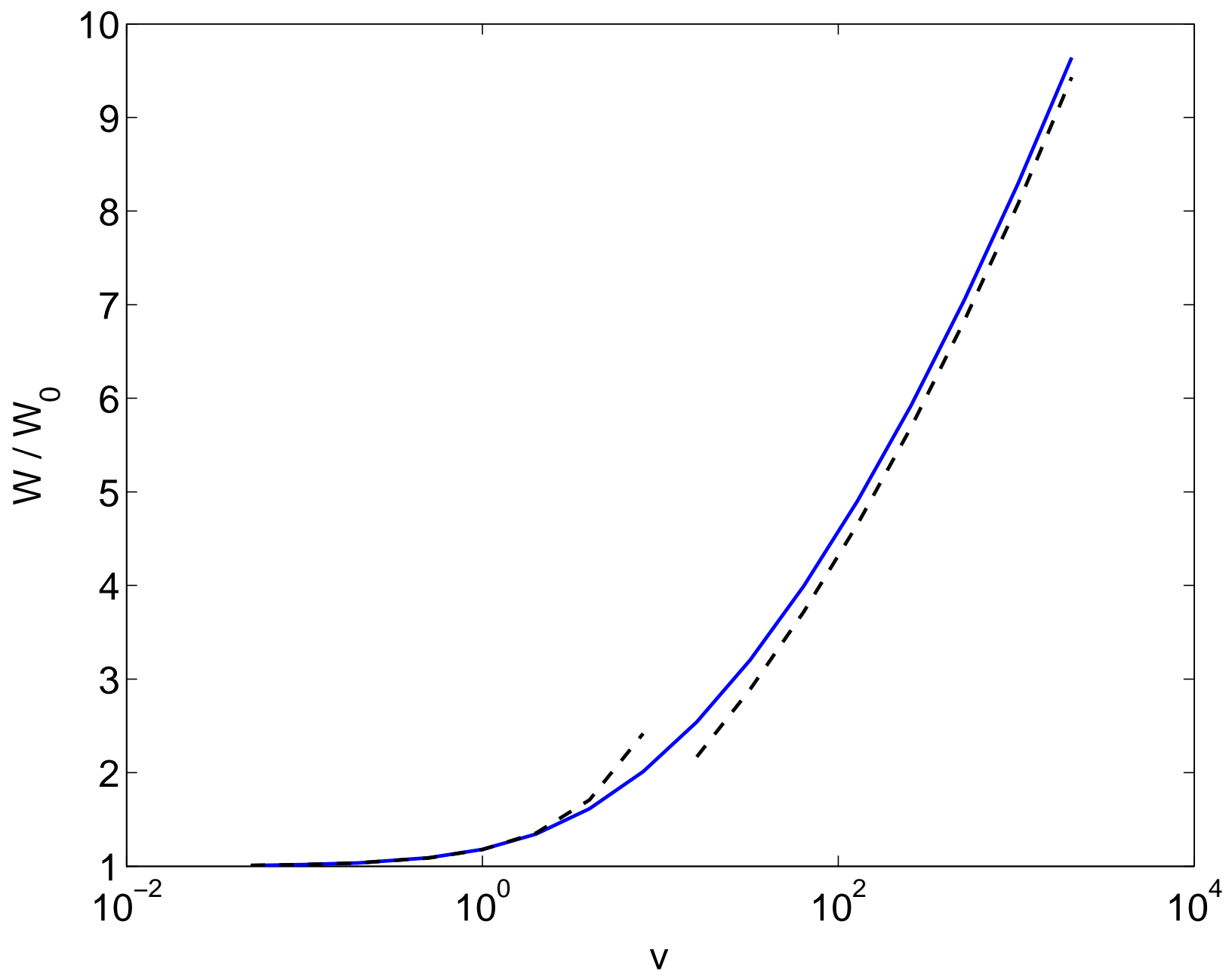


Figure4
[Click here to download Figure: W_vs_v_exp.eps](#)

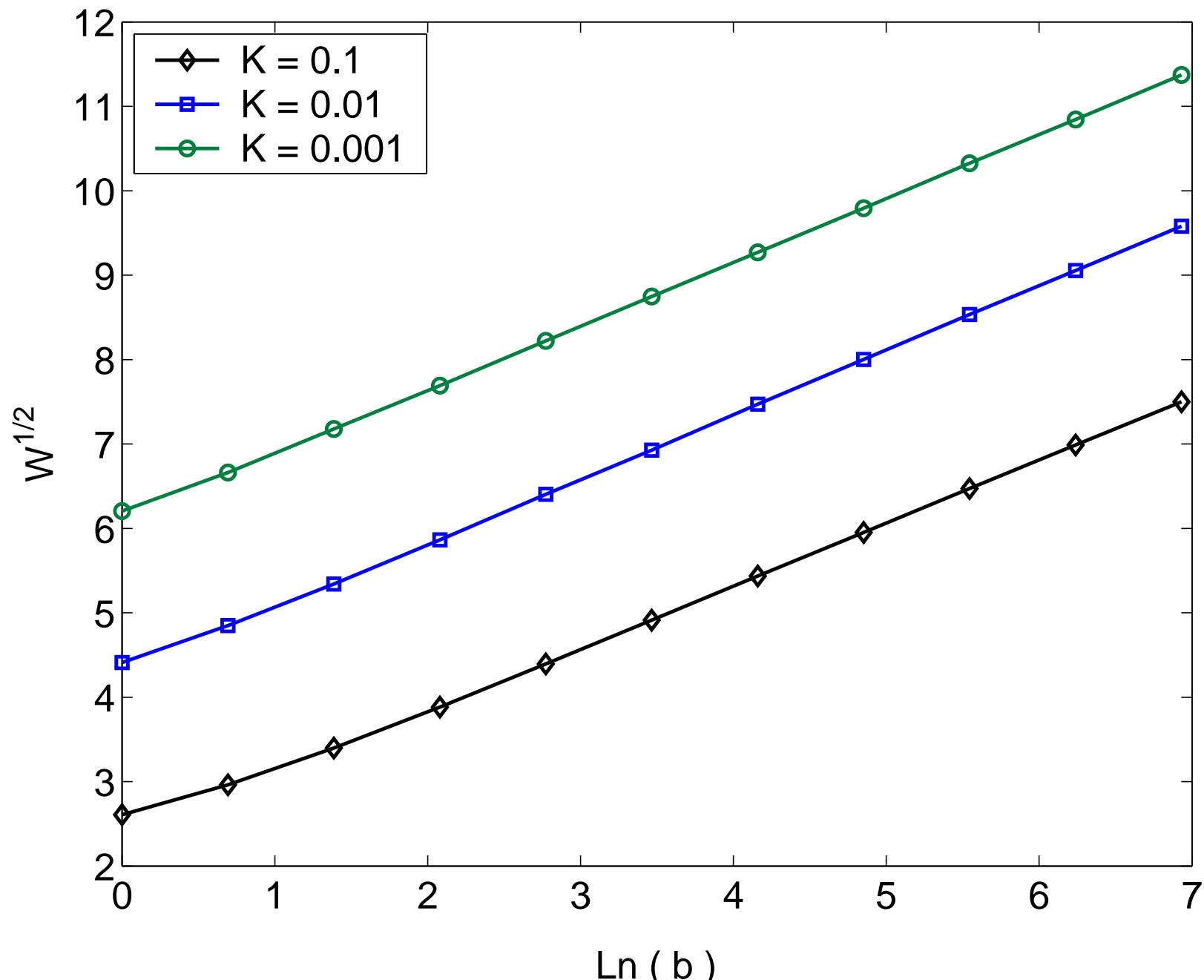


Figure5
[Click here to download Figure: peel.eps](#)

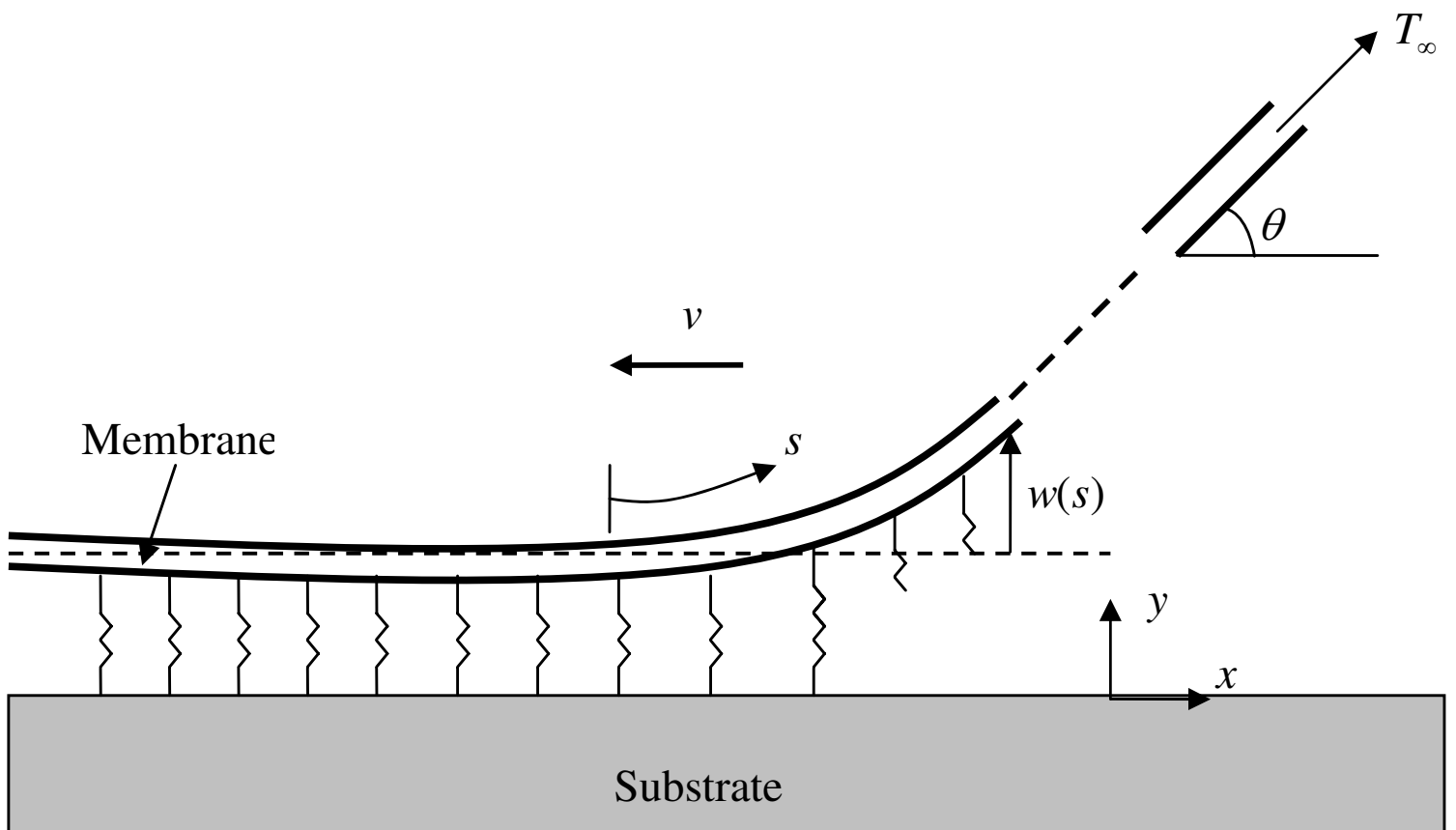


Figure6
[Click here to download Figure: deflection.eps](#)

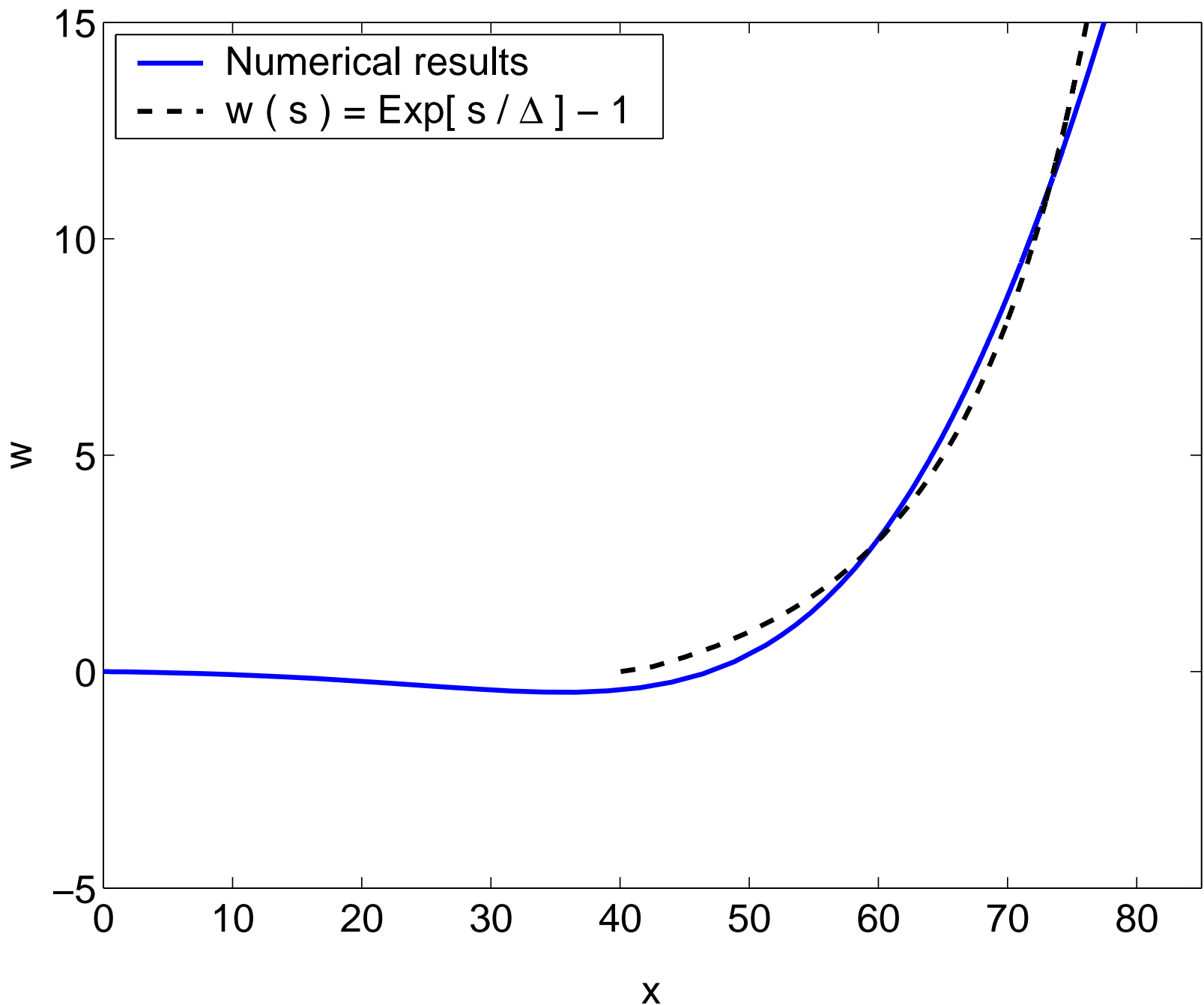


Figure7
[Click here to download Figure: TenBond.eps](#)

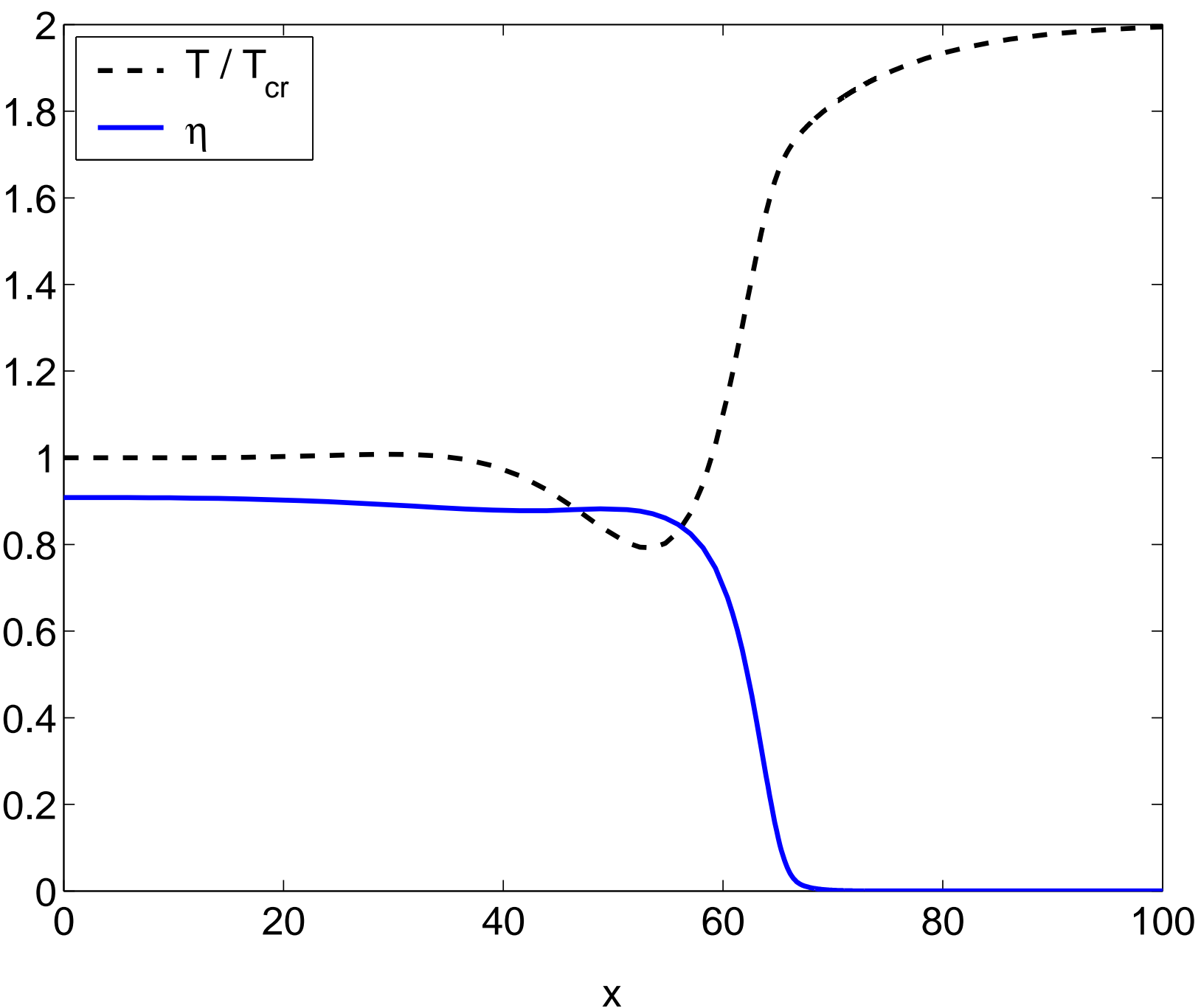


Figure8
[Click here to download Figure: ten_vs_vel.eps](#)

